Quantitative Neutron Resonance Transmission Imaging for archaeometallurgy: calibration using binary bronze alloys within the CHNet_BRONZE Project

Published by IOP Publishing for Sissa Medialab

Received: *January 31, 2026*
Revised: *April 20, 2026*
Accepted: *May 12, 2026*
Published: *June 12, 2026*

International Workshop on Imaging
Milano-Bicocca University, Italy
22–25 September 2025

Quantitative Neutron Resonance Transmission Imaging for archaeometallurgy: calibration using binary bronze alloys within the CHNet_BRONZE Project

G. Marcucci[a,b,*] **M. Clemenza**,[a] **L. Vigorelli**,[a] **F. Grazzi**,[c] **F. Cantini**,[c] **A. Re**,[d,e] **M. Marabotto**,[e] **M. Dematteis**,[d,e] **A. Scherillo**[b] **and D. Di Martino**[a]

[a] *University of Milano-Bicocca, Physics Department, and INFN Sezione di Milano-Bicocca, Milan, Italy*
[b] *STFC ISIS Neutron and Muon Source, Rutherford Appleton Laboratory, Didcot, U.K.*
[c] *CNR, Istituto di Fisica Applicata Nello Carrara, and INFN Sezione di Firenze, Firenze, Italy*
[d] *Dipartimento di Fisica, Università degli Studi di Torino, Torino, Italy*
[e] *INFN Sezione di Torino, Torino, Italy*

E-mail: giulia.marcucci@unimib.it

Abstract: Traditional metallurgical studies of archaeological bronzes often rely on invasive methods, such as metallography or SEM analysis on cross-sections. On the other hand, neutron-based techniques offer unmatched advantages for the non-invasive study of precious artefacts. The CHNet_BRONZE Project aims to develop a complete non-invasive quantitative protocol exploiting neutron absorption and scattering methods available at the ISIS Neutron and Muon Source (U.K.). Their transition to fully quantitative tools optimised for historical copper-based alloys is the core of the project. Neutron Resonance Transmission Imaging (NRTI) has previously demonstrated its potential for elemental identification and semi-quantitative analysis. However, its application as a robust quantitative imaging tool for complex copper-based alloys is still limited by the lack of dedicated calibration strategies and by matrix-dependent effects. In this work, we present a systematic calibration approach for NRTI based on a set of custom-engineered binary Cu-Sn alloys (3–18 wt% Sn), specifically designed to reproduce the compositional range of archaeological bronzes. Our results demonstrate that tin provides a more

*Corresponding author.

https://doi.org/10.1088/1748-0221/21/06/C06010

sensitive and monotonic response to concentration variations, whereas copper resonance dip intensities remain relatively stable, reflecting its role as the matrix reference. This behaviour is also reflected in the selective mapping of the two elements carried out by selecting the resonances: the absorption contrast varies perceptibly for tin depending on its concentration, while it remains almost constant for copper. Therefore, the calibration on binary Cu-Sn alloys has been made using the Sn resonance around 111 eV and shows a good agreement for binary systems. Deviations observed for a multi-component reference alloy highlight the role of matrix effects and the need for further refinement of the method. Overall, this work provides a quantitative baseline for NRTI and represents a key step towards its application as a non-destructive tool for 2D compositional mapping in complex archaeological bronzes, where identifying compositional variations is key to understanding ancient manufacturing processing.

KEYWORDS: Imaging spectroscopy; Inspection with neutrons; Neutron radiography

2026 JINST 21 C06010

Contents

1 **Introduction** 1

2 **Materials and methods** 2

3 **Results** 3

4 **Conclusion** 5

1 Introduction

The metallurgical study of historical copper-based alloys is essential to reconstruct the technological evolution of past civilisations. Conventional archaeometallurgical investigations typically rely on invasive or destructive methods, such as metallography and scanning electron microscopy, which can compromise the integrity of precious cultural heritage objects. To overcome these limitations, the CHNet_BRONZE project, funded by the Italian National Institute of Nuclear Physics (INFN), aims to develop a strictly non-invasive analytical protocol using neutron-based techniques available at the ISIS Neutron and Muon Source. Neutron-based techniques offer significant advantages over conventional non-invasive methods (such as X-rays based techniques) for the study of archaeological metalwork [1]. While X-rays are strongly attenuated by high-density materials, neutrons possess high penetration depth, allowing for the investigation of an artefact's internal bulk through several centimetres of dense alloy. This capability is crucial for archaeological bronzes, which are often covered by corrosion layers (patina) that may yield biased surface-sensitive data. The core of the CHNet_BRONZE project is the quantitative optimisation of three complementary techniques for historical bronzes: Time-of-Flight Neutron Diffraction (ToF-ND) [2], Bragg-Edge Neutron Transmission (BENT) [3], and Neutron Resonance Transmission Imaging (NRTI) [5]. Although these methods are routinely used, their full quantitative exploitation is often hindered by systematic biases, such as resonance saturation, self-shielding effects, and the lack of dedicated refinement parameters for high-Z matrices. Early developments of Neutron Resonance Transmission Imaging at the INES beamline demonstrated the potential of the technique for elemental identification and semi-quantitative analysis, also introducing empirical calibration approaches based on reference samples [4]. However, these approaches remained limited to simplified or empirical correlations and were not designed as systematic calibration protocols for quantitative compositional analysis of complex copper-based alloys, where matrix effects and resonance interactions play a significant role. To address these challenges within historical bronze alloys studies, CHNet_BRONZE exploits a comprehensive set of Cu-based cast alloys. These specimens were engineered within the project to exhibit metallurgical features and microstructures analogous to ancient bronze artefacts, with chemical compositions spanning several material classes: Cu-Sn, Cu-Zn, Cu-Pb, Cu-Sn-Pb, Cu-Zn-Pb, and Cu-Sn-Zn-Pb. The present work focuses specifically on the first systematic attempt to optimise NRTI as a quantitative imaging tool for archaeometallurgical Cu-based alloys using dedicated calibration standards.

2 Materials and methods

The NRTI measurements were carried out at the INES beamline of the ISIS Neutron and Muon Source. This facility provides a pulsed white neutron beam, which is essential for ToF spectroscopy and is exploited by the NRTI technique. The experimental setup utilised a spatial- and time-resolved detector based on the neutron Gas Electron Multiplier technology positioned at a distance of 23.43 m from the neutron moderator. This detector features 0.8 mm of pixel size and a large active area of 10×10 cm^2. However, as the INES beamline provides a maximum beam cross-section of 3.2×3.2 cm^2, the resulting radiographic projections were effectively limited to this size. During the experimental run, each sample was positioned in the neutron hutch perpendicular to the beam, close to the detector. The transmitted neutron flux was recorded in event mode (2D spatial pixels × ToF), enabling a pixel-by-pixel spectroscopic analysis of the bulk material. For the ToF data acquisition, a temporal binning of 1 µs was selected, considering that the ISIS pulse width after moderation is on the order of a few hundred nanoseconds.

A series of five binary bronze (Cu-Sn) and a pure copper specimen, all with a thickness of 4 mm, were produced using metal powders with a micrometric grain size. These standards were specifically engineered to cover the range of tin concentrations most frequently encountered in archaeological metallurgy, typically varying from low-tin bronzes to high-tin alloys. The nominal compositions of the employed cast alloys are summarised in table 1.

Table 1. Nominal elemental composition and areal densities N of the binary bronze (Cu-Sn) calibration specimens.

Cu (wt%)	Sn (wt%)	N_{Cu} (at/b)	N_{Sn} (at/b)	N_{tot} (at/b)
100	0	0.0340	0	0.0340
97	3	0.0327	0.0005	0.0333
94	6	0.0315	0.0011	0.0326
90	10	0.0299	0.0018	0.0317
85	15	0.0279	0.0026	0.0306
82	18	0.0268	0.0031	0.0299

A fundamental step for quantitative analysis is the estimation of the background level. The raw ToF data were first corrected for the background noise using the black resonance method [6]. For this purpose, measurements of the binary alloys with a gold and cobalt/chromium/nickel (Co 42.5/Cr 20/Ni 13/Fe/W/Mo/Mn) filters were performed. Saturated resonances at 4.9 eV (Au), 18.8 eV (W) and 132 eV (Co) were used to fit the time-dependent background, $B(t)$ using a power-law function

$$B(t) = a + b \cdot t^c$$

with parameters determined from the experimental data as $a = 5.312 \times 10^{-3}$, $b = 2.249 \times 10^{-2}$, and $c = -0.326$. The transmission $T(E)$ was then calculated for each specimen as:

$$T(E) = M \frac{C_{in} - B_{in}}{C_{out} - B_{out}}$$

where M is a factor normalising for neutron current determined as described in [7], C_{in} and C_{out} are neutron beam measurements with and without the sample, and B_{in} and B_{out} are the corresponding

2026 JINST 21 C06010

background contributions. Data processing was implemented within the Mantid package [8] to provide an accessible tool to support future users of the INES beamline. The subsequent analysis focused on the main resonance of copper and tin. The goal is to correlate the resonance area, obtained by integrating these dips, with the known Cu and Sn concentration to define a calibration curve for the subsequent quantitative analysis of unknown archaeological bronzes.

3 Results

The transmission spectra obtained from the binary alloys were compared with the total neutron cross-sections from the ENDF/B-VIII.0 databases to identify the most suitable resonances for quantitative analysis (figure 1). The selection criteria focused on peaks that were well-isolated, avoiding cross-overlaps. Other elements or impurities were not detected. As shown in figure 1, the analysis focused on the 111 eV resonance for tin and the 578 eV resonance for copper. The resonance intensity variations of the two elements reflect the relative concentration changes: since Sn increases by a factor of 6 (a relative variation of 500%, from 3wt% to 18wt%), its dip depth shows a strong correlation with the nominal concentration (figure 1(a)). Conversely, because Cu remains the dominant matrix and decreases only from 97 wt% to 82 wt% (relative variation of about 15.5%), its resonance area shows a much less pronounced variation across the different samples (figure 1(b)). To maximise the signal-to-noise ratio, the data extraction was performed by averaging the transmission spectra over a fixed-size region of interest (ROI) for each sample, rather than relying on single-pixel statistics. The epithermal radiographs (figure 2) reveal that several samples exhibit localised density inhomogeneities and internal voids arising from the casting process. Therefore, smaller and homogeneous ROI (2.6 cm^2) have been selected for transmission extraction to ensure the calibration was based on the true material bulk.

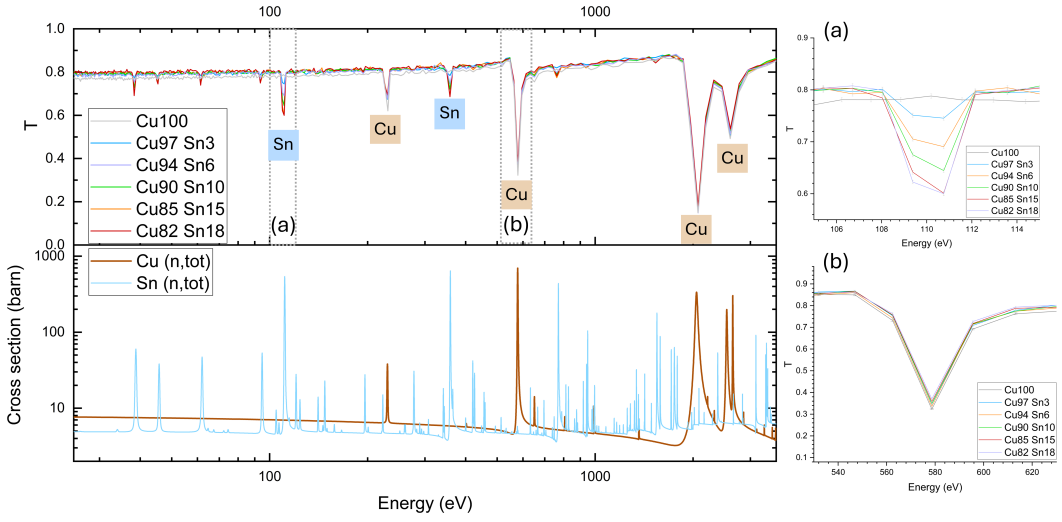

Figure 1. Comparison between normalised transmission spectra of the binary alloys and the total neutron cross-sections from the ENDF/B-VIII.0 database. The analysis focused on two most intense and well-isolated resonances: (a) the 111 eV resonance of Sn and (b) the 578 eV resonance of Cu. The background level is negligible compared to the resonance depth. All data were acquired with a proton current of 800 µA.

2026 JINST 21 C06010

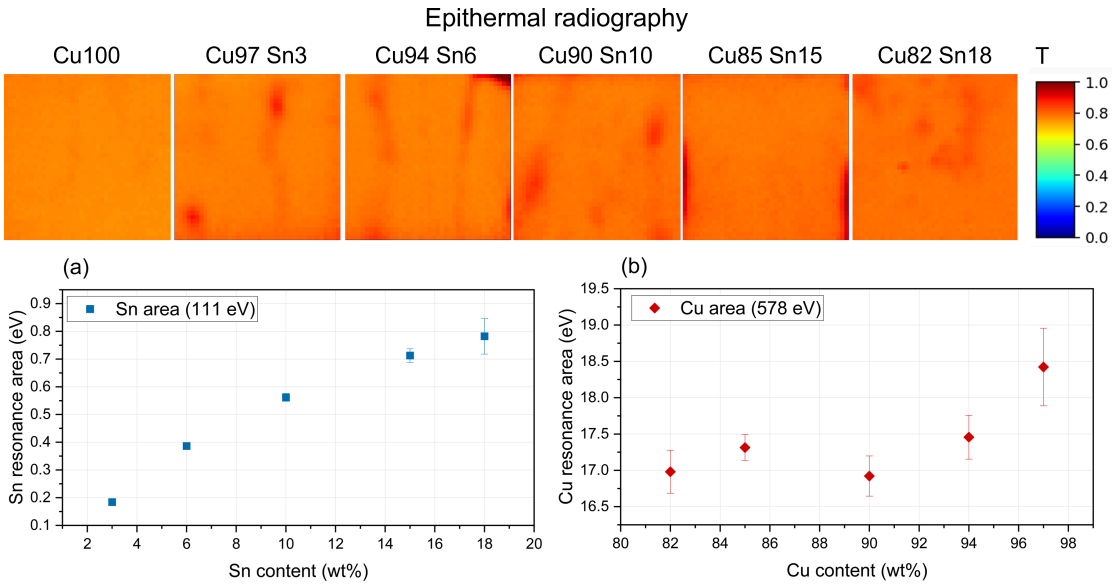

Figure 2. Epithermal radiographs of the binary bronze standards revealing localised density inhomogeneities and internal casting defects (area: 3.2×3.2 cm^2). Panel (a): integrated Sn resonance area at 111 eV as a function of Sn concentration. Panel (b): integrated Cu resonance area at 578 eV as a function of Cu concentration.

Prior to resonance fitting, the transmission spectra were converted to -ln(T(E)), which under the Beer-Lambert approximation is directly proportional to the elemental areal density. The resonance areas were then extracted by fitting the resulting positive peaks with a Voigt function, which accounts for the intrinsic asymmetry of the resonances. Fitting intervals were chosen to ensure sufficient data points for robust estimation of both the resonance profile and the off-resonance level. Accordingly, the integration intervals were defined as 100–120 eV for the 111 eV Sn resonance and 517–650 eV for the 578 eV Cu resonance. The integrated Sn resonance area at 111 eV (figure 2(a)) shows a monotonic increase from 3 wt% to 18 wt% Sn, while the integrated Cu resonance area at 578 eV (figure 2(b)) remains relatively constant across the six alloys, consistent with the small relative variation in copper concentration and confirming its role as a matrix reference. To further compensate for casting-induced inhomogeneities, the calibration curve was constructed by plotting the Sn/Cu resonance area ratio — defined as the ratio of the integrated resonance area of Sn at 111 eV to that of Cu at 578 eV — against the known nominal Sn concentration, rather than the Sn resonance area alone. Under the Beer-Lambert approximation, the local areal density term cancels in the ratio, making the Sn/Cu quantity independent of pixel-wise thickness and density variations. The copper resonance therefore acts as an internal standard for the effective matrix content. The analysis was repeated using the Sn resonance at 357.7 eV and the Cu resonance at 227.5 eV as alternative normalisation references. The 111 eV/578 eV combination yielded the best signal-to-noise ratio and the most stable calibration curve, confirming it as the optimal choice for quantitative analysis in this energy range.

As shown in figure 3, the relationship is well-described by a second-order polynomial curve, $y = a_0 + b_1 x + b_2 x^2$, where a_0 refers to the pure copper sample. This behaviour is consistent with two physical effects operating in the Cu-Sn system. First, as the tin content increases, the FCC lattice parameter of the alloy expands progressively due to the larger atomic radius of Sn with respect to Cu (15% difference, at the upper limit for substitutional alloy formation) [9]. Following Vegard's

2026 JINST 21 C06010

law [10], this lattice expansion — directly measured by neutron diffraction on analogous Cu-Sn cast alloys at the same INES beamline [2] — increases the unit cell volume and consequently reduces the atomic number density of the alloy at constant geometric thickness. As a result, the effective areal density of Sn atoms traversed by the neutron beam grows sub-linearly with increasing Sn weight fraction, producing the negative curvature observed in the calibration. The behaviour of the Sn/Cu plot may suggest that multiple scattering and self-shielding effects also may contribute to the observed sub-linearity. These systematic effects are well documented for NRTA of metallic samples [11]. Future work will explore quantitative corrections for multiple scattering and self-shielding through dedicated Monte Carlo simulations and dedicated resonance shape analysis tools.

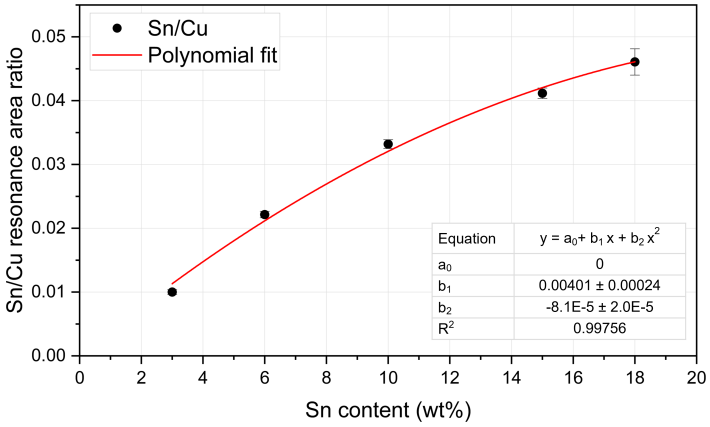

Figure 3. Calibration curve for quantitative tin determination in Cu-Sn alloys. The ratio of the Sn resonance area (111 eV) to the Cu resonance area (578 eV) is plotted against the nominal Sn concentration (wt%).

4 Conclusion

In this work, a first semi-quantitative calibration protocol for NRTI was established for binary Cu-Sn alloys at the INES beamline of the ISIS Neutron and Muon Source. By producing cast binary reference samples, specifically engineered for both neutron diffraction and elemental analysis, the study shows that the 111 eV Sn resonance is a sensitive indicator of tin concentration variations, both in resonant signal and in mapping, while the 578 eV Cu resonance serves as an effective matrix reference. The optimisation procedure took into account biases arising from localised thickness variations and casting inhomogeneities, as these effects are clearly visible on the epithermal radiographs of most of the cast alloys. Despite this mitigation, the calibration showed a measurable curvature, well-described by a second-order polynomial, consistent with the progressive lattice expansion predicted by Vegard's law and self-shielding effects. These results underscore the need for improved accuracy during the resonance fitting process. Such requirements are consistent with other investigations into the impact of systematic effects on the accuracy of neutron resonance transmission analysis, which have highlighted how instrumental response and resonance parameters influence the final areal density calculations [11]. Consequently, the next stage of the project will focus on integrating more specialised analysis tools into the quantitative optimisation of NRTI at the ISIS facility. Overall, this research establishes a starting point for further NRTI technical optimisation from a qualitative technique to a fully quantitative imaging tool for the non-destructive study of complex archaeological Cu-based artefacts, with the outlook of extending future calibration models to ternary and quaternary alloys.

2026 JINST 21 C06010

Acknowledgments

We acknowledge the Italian Institute of Nuclear Physics (INFN) - CSN 5 for financial support via the CHNet_BRONZE experiment. Experiments at the ISIS Neutron and Muon Source were supported by beamtime allocation RB2500010 from the Science and Technology Facilities Council (data: https://doi.org/10.5286/ISIS.E.RB2500010).

References

[1] N. Kardjilov and G. Festa, *Neutron Methods for Archaeology and Cultural Heritage*, Springer (2017) [DOI:10.1007/978-3-319-33163-8].

[2] F. Grazzi, L. Bartoli, S. Siano and M. Zoppi, *Characterization of copper alloys of archaeometallurgical interest using neutron diffraction: a systematic calibration study*, *Anal. Bioanal. Chem.* **397** (2010) 2501.

[3] M. Marabotto, et al., *Preliminary evaluation of calibration method on Double Crystal Monochromator and Time-of-Flight Bragg Edge Neutron Transmission analysis*, *Nuovo Cim. C* **48** (2025) 242.

[4] E.P. Cippo et al., *Imaging of cultural heritage objects using neutron resonances*, *J. Anal. At. Spectrom.* **26** (2011) 992.

[5] G. Marcucci, A. Scherillo, D. Raspino and D. Di Martino, *Isotopic imaging with epithermal neutrons at the ISIS Neutron and Muon Source*, *Sci. Rep.* **15** (2025) 19344.

[6] P. Schillebeeckx et al., *Determination of Resonance Parameters and their Covariances from Neutron Induced Reaction Cross Section Data*, *Nucl. Data Sheets* **113** (2012) 3054.

[7] G. Marcucci, *The normalisation workflow and post-processing pipeline for Neutron Resonance Transmission Imaging at the INES beamline*, 2026 *JINST* **21** C04074.

[8] O. Arnold et al., *Mantid — Data analysis and visualization package for neutron scattering and μ SR experiments*, *Nucl. Instrum. Meth. A* **764** (2014) 156 [arXiv:1407.5860].

[9] D.A. Scott et al., *Metallography and Microstructure of Ancient and Historic Metals*, Marina del Rey, CA: Getty Conservation Institute in association with Archetype Books (1991) [http://hdl.handle.net/10020/gci_pubs/metallography_microstructure].

[10] L. Vegard, *Die Konstitution der Mischkristalle und die Raumfüllung der Atome*, *Z. Phys.* **5** (1921) 17.

[11] H. Tsuchiya et al., *Impact of systematic effects on results of neutron resonance transmission analysis*, *Nucl. Instrum. Meth. A* **767** (2014) 364.

2026 JINST 21 C06010